Advance Publication

Experimental Animals

Received: 2022.2.10

Accepted: 2022.4.13

J-STAGE Advance Published Date: 2022.5.13

Categories: Immunology

Original paper

The establishment and application of CD3E humanized mice in immunotherapy

Running Head: CD3E humanized mice and immunotherapy

Rufeng Zhang[#1], Jing Zhang[#2], Xiaofei Zhou[2], Ang Zhao[2], Changyuan Yu[†,1]

[1]College of life science and technology, Beijing University of Chemical Technology, Beijing, China

[2] Biocytogen Pharmaceuticals (Beijing) Co., Ltd, Beijing, China.

[#] :These authors contributed equally to this work

[†]Corresponding Author

Changyuan Yu

Beijing University of Chemical Technology

15 Beisanhuan East Road, Chaoyang District, Beijing

Email: yucy@mail.buct.edu.cn

Abstract

In the field of cancer immunotherapy, monoclonal antibody drugs, bispecific antibodies, and antibody-conjugated drugs have become the focus of current research, and gene-edited animal models play an essential role in the entire drug development process. In this study, CD3E humanized mice were established by replacing the second to the seventh exon of the *Cd3e* mouse gene with the same exon of the human gene. The expression of human CD3E in CD3E humanized mice was detected by RT-PCR as well as flow cytometry, also a tumor model was established based on CD3E humanized mice, and the pharmacodynamic effects of CD3E monoclonal antibodies were evaluated. The results showed that CD3E humanized mice expressed only human CD3E, and the proportion of each lymphocyte in the thymus and spleen was not significantly changed compared with wild-type mice. CD3E monoclonal antibody could promote tumor growth after treatment, which may be related to the activation-induced cell death effect caused by this CD3E antibody. In contrast, Bispecific antibody blinatumomab inhibited tumor growth significantly. Thus, the CD3E humanized mice provided an adequate animal model for evaluating the efficacy and safety of CD3E antibody drugs.

Key words: CD3E； humanized mouse model； monoclonal antibody； Immunotherapy

1. Introduction

The TCR-CD3 complex, which is present on the surface of T lymphocytes, plays an essential role in the adaptive immune response. This complex is formed by CD3δ, CD3ε, CD3γ, and CD3ζ, together with T cell receptor α/β or γ/δ heterodimers. When antigen-presenting cells (APCs) activate the T-cell receptor (TCR), TCR-mediated signals are transmitted across the cell membrane via the CD3 chains CD3δ, CD3ε, CD3γ, and CD3ζ [1, 2]. The cytoplasmic regions of all CD3 chains contain immunoreceptor tyrosine-activated motifs (ITAMs). Upon TCR binding, these motifs are phosphorylated by the Src family protein tyrosine kinases LCK and FYN, leading to activation of downstream signaling pathways [3, 4]. Among the subunits of these constituent complexes, CD3ε plays an essential role in T-cell development through the formation of two heterodimers CD3δ/CD3ε and CD3γ/CD3ε, to initiate the assembly of the TCR-CD3 complex [5, 6]. CD3δ, CD3γ, and CD3Z deficient mice do not entirely prevent this process, although they all inhibit T cell maturation and TCR expression to varying degrees [7-9]. In contrast, CD3ε knockout mice are unable to assemble the TCR precursors TCRα/β or γδTCR and thus lack mature T cells [10, 11].

Antibody drugs are gradually playing an increasingly important role in the new era of tumor immunotherapy [12, 13]. Due to interspecies differences, many antibodies cannot be carried out directly using mice for preclinical experiments. Immune reconstitution using nude mice is a critical way to solve this problem. Although immune reconstitution can reconstruct the human immune system to some extent [14, 15], some immune cells are still not able to develop [16, 17].

Genetically modified target humanized mouse models are an effective way to address interspecies differences [18]. In this study, we established a humanized CD3E mice by replacing

the murine *Cd3e* gene with the human *CD3E* gene. The humanized CD3E mice can be used as an effective tool for the efficacy evaluation of CD3E-targeted drugs and toxicological evaluation.

2. Material and methods

2.1 Animal experiments

C57BL/6N mice were purchased from Beijing Vital River Laboratory Animal Technology Co. Ltd. CD3E humanized (B-hCD3E) mice were provided by Biocytogen Pharmaceuticals (Beijing) Co., Ltd, production license No. SCXK (Su) 2016-0004. All animal studies were performed according to the protocol approved by the animal care and use committee of Biocytogen Pharmaceuticals. The experimental animals were housed in the SPF barrier facility with a controlled temperature (22 ± 2℃), a 12 h/12 h light/dark cycle, and were free access to food and water. Mice were euthanized by CO_2 inhalation at the end of the experiment.

2.2 Generation of B-hCD3E mice

On the C57BL/6J genetic background, a contiguous mouse genomic sequence of approximately 8.3 kb at the endogenous mouse *Cd3e* locus as deleted and replaced with approximately 8.8 kb of human *CD3E* genomic sequence comprising exon 2 starting from the the ATG initiation codon (ATG) through exon 7 ending to the D126 codon (GAT) of the human *CD3E* gene. The hCD3E targeting vector was designed to contain homology regions, human DNA, Frt-flanked Neo resistance cassette and diphtheria toxin A (DTA) cassette. The mouse and human genomic DNA fragments from relevant BAC clone were cloned to the vector pL451 (Biocytogen Pharmaceuticals (Beijing) Co., Ltd) to form an intermediate vector, which contained Frt-flanked Neo resistance cassette. The BAC clones from C57BL/6J mouse genomic BAC library were modified with PmlI (hCD3E) intermediate vector fragment by homologous recombination. These modified BACs were used to construct the targeting vectors. The targeting vector contains a diphtheria toxin A (DTA) cassette. The DTA gene was used for negative selection of clones with

random integration. The targeting vectors were linearized before they were transfected into C57BL/6J embryonic stem (ES) cells (Biocytogen Pharmaceuticals (Beijing) Co., Ltd) by electroporation respectively. The G418-resistant ES clones were screened for homologous recombination by PCR. Correctly targeted clones were confirmed by Southern blot analysis with probes. Confirmed clones were injected into BALB/c blastocysts and implanted into pseudo pregnant females to generate chimeric mice. Chimeric mice were bred to Flp mice to obtain F1 mice carrying the recombined allele containing the deleted-neo allele.

2.3 Reagents and materials

MC38(colon adenocarcinoma) cells were purchased from ShunRan biology and were grown and maintained in Dulbecco's Modified Eagle's medium (DMEM) containing 10% fetal bovine serum (FBS) at 37℃ and 5% CO_2. To construct MC38 overexpressing human CD19 cell line (MC38-hCD19), the exogenous promoter and human CD19 coding sequence was inserted to replace part of murine exon 2 and all of exons 3~12. Antibodies against mouse cell-surface molecules including mCD45-PE-Cy7 (clone HI30, USA), mCD4-BV421 (clone GK1.5, USA), mCD8-BV711 (clone 53−6.7, USA) mCD19-APC-Cy7 (clone 6D5, USA), mNK1.1-PE-Cy7 (clone PK136, USA), mCD11c-BV605(clone N418, USA), mCD11b-PE (clone M1/70, USA), mGr1-APC (clone RB6−8C5, USA), mF4/80-FITC (clone 8M8, USA), mCD3E-PerCP (clone 145-2C11) , mCD69-APC-(clone H1.2F3), mCD25-APC-(clone BC96), and anti-human hCD3E-PerCP (clone UCHT1) were purchased from Biolegend. mFoxp3-PE（clone FJK-16s, USA） were purchased from Invitrogen. mTCRβ-APC (clone H57-597, USA) antibody was purchased from BD Bioscience. ACK Lysis Buffer was purchased from Beyotime (C3702, China). The mouse IFN-γ ELISA Kit was purchased from Biolegend, The HTRF mouse IL2 kit was from Cisboi. The anti-human CD3E monoclonal antibody (hCD3E), anti-mouse CD3E monoclonal

antibody (mCD3E) and anti-mouse PD-1 monoclonal antibody (mPD-1) for in vivo efficacy were provided by Biocytogen Pharmaceuticals (Beijing) Co., Ltd.

2.4 Analysis of human CD3E protein expression and cluster of immune cells

Spleen and thymus of C57BL/6N mice and B-hCD3E mice were collected under aseptic conditions and weighed, then the spleen and thymus were placed on a 70 μm sieve, ground with 6 mL of PBS, centrifuged at 2000 rpm for 5 min at 4 ℃, and the supernatant was discarded. The erythrocytes were removed by ACK Erythrocyte Lysis Solution. The reaction was terminated by adding 8 mL of PBS, and the supernatant was discarded after centrifugation at 2000 rpm for 5 min at 4 ℃. The obtained splenocytes and thymocytes were incubated with fluorescent direct labeling antibodies for 30 min at 4 ℃, protected from light, washed with PBS, and resuspended before being analyzed using flow cytometry.

2.5 T cell proliferation, differentiation and cytokine level detection in vitro

The obtained spleen cells were sorted by magnetic beads to obtain T cells. 300μL of CSFE staining solution with a final concentration of 5μM was added to 300μL of cell suspension, mixed well, and incubated for 5min at room temperature and protected from light for staining. The staining was terminated by adding 9mL of 1640 complete medium, then the cells were centrifuged at 4℃ for 2000 rpm for 3min, and the supernatant was discarded. Cells were resuspended using 10 mL of 1640 complete medium, counted, and the cell concentration was adjusted to 2.5×10^6/mL. 96-well plates were coated with Anti-mCD3E (2 μg/mL) and Anti-hCD3E (2 μg/mL), respectively, and incubated with Anti-mCD28 (5 μg/mL) at 37°C for 2 hours. 5×10^5 CFSE-stained T cells per well were placed in the coated 96-well plates and incubated for 24, 48, and 72 h before being analyzed using flow cytometry. Cell culture supernatants were collected, and cytokine IL-2 and IFN-γ levels were detected.

2.6 In vivo efficacy of CD3E antibodies

5×10^5 MC38 cells were inoculated into the flank of female C57BL/6N mice and CD3E humanized mice, and the mice were grouped when the tumors grew to approximately 100 mm^3. For the monoclonal antibodies treatment, C57BL/6N mice and humanized mice were randomly grouped according to tumor volume, as the saline solvent control group, mPD-1 Ab (10 mg/kg) group, hCD3 Ab (2 mg/kg) group, and mCD3 Ab (2 mg/kg) group. The antibodies were administered twice a week for 5-6 consecutive doses. For the bispecific antibody treatment, MC38-hCD19 cells were implanted subcutaneously into B-hCD3E mice, then the mice were grouped as the saline solvent control group, low-dose (0.03ug/mouse), middle-dose (1ug/mouse), and high-dose (10ug/mouse) groups of Blinatumomab. The body weight and tumor volume of the mice were measured twice a week during the administration and the observation period. At the end of the experiment, the animals were euthanized, and the relative tumor growth inhibition rate (TGI) was calculated.

2.7 Detection of T cells in peripheral blood of mice after CD3 antibody administration

Forty-eight hours after the first antibody administration, 100 μL of peripheral blood was collected from each mouse and lysed for 5 min using ACK red blood cell lysis solution to remove red blood cells. The reaction was terminated by adding 8 mL of PBS, and the supernatant was discarded after centrifugation at 2000 rpm for 5 min at 4 ℃. After resuspension of cells using PBS, the obtained lymphocytes were incubated with the fluorescent direct-labeled antibody for 30 min at 4 ℃, protected from light, washed with PBS, and resuspended before being analyzed using flow cytometry.

2.8 Statistical analysis

Data are expressed as means ± SEM. a Student's t-test was applied to determine the statistical significance. A value of $P < 0.05$ was considered statistically significant.

3 Results

3.1 Generation of humanized CD3E mice

Due to the interspecies difference between human and murine CD3 subunits, it is impossible to evaluate the efficacy of targeting CD3 drugs using wild-type mice. In this study, the exon 2 to exon 7, which encodes the signal peptide and extracellular region of mCD3E, was replaced by the region of hCD3E to generate chimeric CD3E protein with a murine-derived intracellular region (Figure 1A). RT-PCR results showed that mouse *Cd3e* mRNA was detectable only in splenocytes of wild-type while human *CD3E* mRNA was detectable only in homozygous B-hCD3E mice (Figure 1B).

After obtaining CD3E humanized mice, spleens of mice were collected, and splenocytes were isolated, and the expression of human CD3E protein was detected by flow cytometry. The results showed that in wild-type mice, 18.7% of the cells expressed mCD3E protein after detection by anti-mouse CD3E antibody; and in CD3E humanized mice, 22.1% of cells expressed human CD3E protein while mouse CD3E protein was not expressed after detection by anti-human CD3E antibody (Figure 1C).

3.2 Basal characteristics of CD3E humanized mice

It has been reported that thymocytes are deficient in human CD3E transgenic mice. The degree of deficiency is related to the transgene copy number, with a higher copy number leading to increased T-cell deficiency [4]. In this study, the thymus and spleen of CD3E humanized and wild-type mice were collected and weighed separately. The results showed that the morphology of the spleen and thymus of CD3E humanized mice did not differ significantly from that of wild-type

mice, and both remained intact (Figure 1D). Compared with wild-type mice, there was no significant change in spleen- body weight ratio in CD3E humanized mice; however, the thymus weight in B-hCD3E mice is slightly lower than that of WT C57BL/6 mice (Figure 1D, E).

3.3 Immune cell and T cell subpopulation distribution in CD3E humanized mice

Next, we further isolated spleen cells from CD3E humanized mice and C57BL/6N mice, respectively, and detected the distribution of each lymphocyte in both mice by flow cytometry. The results showed that the proportions of B cells, T cells, NK cells, DC cells, granulocytes, macrophages, and monocytes cells in the spleen cells of CD3E humanized mice after humanization were 65.0%, 23.6%, 5.23%, 2.96%, 0.52%, 1.89%, and 1.62% of CD45+ cells, which were consistent with the distribution in wild-type mice (Figure 2).

We further analyzed the distribution of CD4 T cells, CD8 T cells, and Treg cells in T cells. The proportions of CD4+ cells, CD8+ cells among TCRβ+ cells were 62.5%, 24.2% respectively, while the proportion of Foxp3+ cells among CD4+ cells was 3.65% in CD3E humanized mice, this result was not significantly different from the distribution of each cell type in wild-type mice (Figure 3A-B). The above results were similarly verified in spleen cells (Figure 3C-D).

Together, the above results indicate that CD3E humanization modification does not affect the distribution of each lymphocyte subpopulation, especially the T-cell subpopulation in mice.

3.4 T-cell proliferation and activation in CD3E humanized mice

We further investigated the effect of CD3E humanization on T cell function. T lymphocytes (2.5×10^6 cells) isolated from the spleen of C57BL/6 mice and CD3E humanized were stimulated by using Anti-mCD3E and Anti-hCD3E co-stimulated with Anti-mCD28, respectively. Flow cytometry assays of T cell proliferation and activation showed that in B-hCD3e mice, only anti-hCD3 stimulated T cell proliferation, whereas in C57BL/6 mice only anti-mCD3 stimulated T cell

proliferation, and the proportion of proliferation in B-hCD3e mice was similar to that in C57BL/6 mice (Figure 4A-B). Similarly, the activation of CD25 and CD69-labeled T cells showed the same pattern as T cell proliferation (Figure 5A-B).

IFN-γ and IL-2 were detected by ELISA after 24, 48, and 72 h to reflect T cell proliferation and activation. The results showed that concentration of IFN-γ and IL-2 in B-hCD3E mice was similar to that of C57BL/6 mice, indicating that CD3E humanization in B-hCD3E mice does not change the cytokine secretion after T cell activation (Supplementary Figure 1).

3.5 Effect of CD3E antibodies on tumorigenesis in mice

To further investigate the application of CD3E humanized mice in cancer immunotherapy, a cell line-derived syngeneic model was performed on CD3E humanized mice and wild-type mice. In wild-type C57BL/6 mice, the PD-1 antibody administration group showed a significant reduction in tumor volume, but the murine CD3E antibody group showed a significant increase in tumor volume. The tumors in the anti-human CD3E antibody group (Teplizumab) were close to the control group, indicating that in wild-type mice, only the murine CD3E antibody could support tumor cell growth (Figure 6A). Further analysis of T- and B-cell ratios revealed that TCRβ% was significantly lower in the murine CD3E antibody group than in the other groups (data not shown).

In CD3E humanized mice, the results of tumor volume in the control and PD-1 administration groups were consistent with the previous experiments, and treatment with human CD3E antibody Teplizumab showed a significant increase in tumor volume. The tumor volume after treatment with murine CD3E antibody was not significantly different from the control group, indicating that anti-human CD3E antibody Teplizumab in humanized CD3E mice better support the growth of tumor cells (Figure 6B). Further analysis of the ratio of T cells and B cells in the peripheral blood cells of these mice revealed no significant difference in the ratio of B cells (Fig 7A). While the

proportion of T cells was significantly lower in anti-human CD3E antibody treatment group (Fig 7B). Moreover, the proportion of $CD4^+$ T cells and $CD8^+$ T cells in this group of mice was also significantly lower than that in the control group (Fig 7C-D).For the results of Blinatumamab, the tumor volume can be suppressed by Blinatumamab dose-dependently (Figure 6C), indicating that T cells are specifically recruited to the tumor surface by bispecific antibodies Blinatumamab through their surface CD3 complexes.

The above experiments showed that the humanized CD3E mice generated by this method have normal immune responses, can effectively bind human CD3E antibody and transduce downstream signals, which proved that the humanized CD3E mice can be used for screening anti-human CD3E antibody and in vivo drug efficacy assay, and can be used as an in vivo alternative model for in vivo studies for the screening, evaluation, and treatment of human CD3E signaling pathway regulators, bispecific antibodies and other drugs.

4. Discussion

In the present study, we successfully established CD3E humanized mice by replacing the murine CD3E extracellular region with human CD3E extracellular region through gene targeting technique. The distribution of lymphocyte subpopulations in the thymus and spleen of this mouse was consistent with that of wild-type mice, indicating that humanized mice did not affect the distribution of lymphocyte subpopulations. The proliferation and activation of T cells in CD3E humanized mice isolated from the thymus and spleen under co-stimulation with CD3 and CD28 were consistent with those in wild-type mice, indicating that humanized mice do not affect the proliferation and activation of T cells.

CD3E humanized mouse has been reported in some cases, and overexpression of the human *CD3E* gene in wild mice has limited the application of this mouse due to the high copy number of

CD3E expression, which causes abnormal thymus development [19] . Our humanized mice were generated by replacing the mouse extracellular region sequence with the human CD3E extracellular region sequence. The mice had normal spleen development. Although the thymus to body weight ratio was decreased, further analysis revealed that the ratio of CD4, CD8 cells to Treg cells in the thymus of these mice was similar to wild type. The proliferation and activation of T cells were not significantly different from those of wild-type mice, indicating the normal function of the humanized mice.

We observed a significant increase in tumor volume in the MC38 syngeneic tumor mouse model in wild-type mice and human CD3E humanized mice administered with mouse and human CD3E antibodies, respectively. To investigate the mechanism behind this phenomenon, we found that in humanized mice, the proportion of T cells in peripheral blood was significantly lower in anti-human CD3E antibody-treated mice than that of controls. Activation-induced cell death (AICD) is the process of programmed cell death of thymocytes by apoptosis of matured T cells, which can be induced by CD3E antibody [20, 21]. We therefore speculate that the decrease in T cells and increase in tumor volume after treatment of CD3E antibody in our experiments may be caused by AICD, but further experimental evidence is still needed to prove this assumption.

The development of CD3E antibody drugs has been much studied in many disease areas such as oncology, infection, immune rejection, and type 1 diabetes, in the form of drugs including monoclonal antibodies, bispecific antibodies, and CAR-T, indicating the great importance of drug research against CD3E targets [22-26]. The CD3E humanized mice generated in this study are of great importance for the drug development and immunological mechanisms of this target in tumor and autoimmune diseases [19, 27].

Author contributions

Rufeng Zhang, Jing Zhang, Xiaofei Zhou, Ang Zhao designed and performed the experiments; Rufeng Zhang, Jing Zhang and Changyuan Yu analyzed data and wrote the manuscript.

Conflict of Interest

This research was conducted with a research fund from Beijing University of Chemical Technology, which the primary author Rufeng Zhang and corresponding author Changyuan Yu belongs to. Jing Zhang, Xiaofei Zhou, Ang Zhao are employees of Biocytogen Pharmaceuticals (Beijing) Co., Ltd.

Sources of founding

This work was supported by National Natural Science Foundation of China (Grant No. 82174531).

References

1. Dong, Zheng L, Lin J, Zhang B, Zhu Y, Li N, et al. Structural basis of assembly of the human T cell receptor-CD3 complex. Nature. 2019;573(7775):546-52.
2. Call ME, Wucherpfennig KW. Molecular mechanisms for the assembly of the T cell receptor-CD3 complex. Mol Immunol. 2004;40(18):1295-305.
3. Barber EK, Dasgupta JD, Schlossman SF, Trevillyan JM, Rudd CE. The CD4 and CD8 antigens are coupled to a protein-tyrosine kinase (p56lck) that phosphorylates the CD3 complex. Proc Natl Acad Sci U S A. 1989;86(9):3277-81.
4. Alarcon B, Gil D, Delgado P, Schamel WW. Initiation of TCR signaling: regulation within CD3 dimers. Immunol Rev. 2003;191:38-46.
5. Borroto A, Lama J, Niedergang F, Dautry-Varsat A, Alarcon B, Alcover A. The CD3 epsilon subunit of the TCR contains endocytosis signals. J Immunol. 1999;163(1):25-31.
6. Martin-Blanco N, Jimenez Teja D, Bretones G, Borroto A, Caraballo M, Screpanti I, et al. CD3epsilon recruits Numb to promote TCR degradation. Int Immunol. 2016;28(3):127-37.
7. Dave VP, Cao Z, Browne C, Alarcon B, Fernandez-Miguel G, Lafaille J, et al. CD3 delta deficiency arrests development of the alpha beta but not the gamma delta T cell lineage. EMBO J. 1997;16(6):1360-70.
8. Haks MC, Krimpenfort P, Borst J, Kruisbeek AM. The CD3gamma chain is essential for development of both the TCRalphabeta and TCRgammadelta lineages. EMBO J. 1998;17(7):1871-82.
9. Shores EW, Huang K, Tran T, Lee E, Grinberg A, Love PE. Role of TCR zeta chain in T cell development and selection. Science. 1994;266(5187):1047-50.
10. DeJarnette JB, Sommers CL, Huang K, Woodside KJ, Emmons R, Katz K, et al. Specific requirement for CD3epsilon in T cell development. Proc Natl Acad Sci U S A. 1998;95(25):14909-14.
11. Malissen M, Gillet A, Ardouin L, Bouvier G, Trucy J, Ferrier P, et al. Altered T cell development in mice with a targeted mutation of the CD3-epsilon gene. EMBO J. 1995;14(19):4641-53.
12. Kimiz-Gebologlu I, Gulce-Iz S, Biray-Avci C. Monoclonal antibodies in cancer immunotherapy. Mol Biol Rep. 2018;45(6):2935-40.
13. Thomas A, Teicher BA, Hassan R. Antibody–drug conjugates for cancer therapy. The

Lancet Oncology. 2016;17(6):e254-e62.
14. Aryee KE, Shultz LD, Brehm MA. Immunodeficient mouse model for human hematopoietic stem cell engraftment and immune system development. Methods Mol Biol. 2014;1185:267-78.
15. Rongvaux A, Takizawa H, Strowig T, Willinger T, Eynon EE, Flavell RA, et al. Human hemato-lymphoid system mice: current use and future potential for medicine. Annu Rev Immunol. 2013;31:635-74.
16. Shultz LD, Brehm MA, Garcia-Martinez JV, Greiner DL. Humanized mice for immune system investigation: progress, promise and challenges. Nat Rev Immunol. 2012;12(11):786-98.
17. Manz MG. Human-hemato-lymphoid-system mice: opportunities and challenges. Immunity. 2007;26(5):537-41.
18. Olson B, Li Y, Lin Y, Liu ET, Patnaik A. Mouse Models for Cancer Immunotherapy Research. Cancer Discov. 2018;8(11):1358-65.
19. Wang B, Biron C, She J, Higgins K, Sunshine MJ, Lacy E, et al. A block in both early T lymphocyte and natural killer cell development in transgenic mice with high-copy numbers of the human CD3E gene. Proc Natl Acad Sci U S A. 1994;91(20):9402-6.
20. Liu Y, He Y, Zhang J, Jiang L, Liu S, Zheng D. Tyrosine mutation in CD3epsilon-ITAM blocked T lymphocyte apoptosis mediated by CD3epsilon. Immunol Invest. 2003;32(1-2):59-70.
21. Varadhachary AS, Perdow SN, Hu C, Ramanarayanan M, Salgame P. Differential ability of T cell subsets to undergo activation-induced cell death. Proc Natl Acad Sci U S A. 1997;94(11):5778-83.
22. Sugita S, Shimizu J, Makabe K, Keino H, Watanabe T, Takahashi M. Inhibition of T cell-mediated inflammation in uveitis by a novel anti-CD3 antibody. Arthritis Res Ther. 2017;19(1):176.
23. Bacac M, Fauti T, Sam J, Colombetti S, Weinzierl T, Ouaret D, et al. A Novel Carcinoembryonic Antigen T-Cell Bispecific Antibody (CEA TCB) for the Treatment of Solid Tumors. Clin Cancer Res. 2016;22(13):3286-97.
24. Gaglia J, Kissler S. Anti-CD3 Antibody for the Prevention of Type 1 Diabetes: A Story of Perseverance. Biochemistry. 2019;58(40):4107-11.
25. Shiraiwa H, Narita A, Kamata-Sakurai M, Ishiguro T, Sano Y, Hironiwa N, et al. Engineering a bispecific antibody with a common light chain: Identification and optimization of an anti-CD3 epsilon and anti-GPC3 bispecific antibody, ERY974. Methods. 2019;154:10-20.

26. Wu W, Zhou Q, Masubuchi T, Shi X, Li H, Xu X, et al. Multiple Signaling Roles of CD3epsilon and Its Application in CAR-T Cell Therapy. Cell. 2020;182(4):855-71 e23.
27. Ueda O, Wada NA, Kinoshita Y, Hino H, Kakefuda M, Ito T, et al. Entire CD3epsilon, delta, and gamma humanized mouse to evaluate human CD3-mediated therapeutics. Sci Rep. 2017;7:45839.

Figure legends:

Fig. 1 Generation of CD3E humanized mice

(A) Target strategy of CD3E humanized mice. (B) Strain specific analysis of CD3E gene expression in CD3E humanized mice and C57BL/6 mice by RT-PCR. (C) CD3E proteins expression level in CD3E humanized mice and C57BL/6 mice. (D) Representative photos of thymus and spleen. (E) Weight (% of body weight) of thymus and spleen in CD3E humanized mice and C57BL/6 mice. n=4 mice per group.

Fig.2 Analysis of leukocytes subpopulation in B-hCD3E mice spleen

(A) Flow cytometry pictures of leukocytes subpopulation in CD3E humanized mice and C57BL/6 mice. (B) Percent of T, B, NK, DC, Granulocytes, macrophage and Monocyte cells in spleen leukocyte of CD3E humanized mice and C57BL/6 mice. n=6 mice per group.

Fig. 3 Analysis of thymus and spleen T cell subpopulations

(A) Flow cytometry pictures of thymus T cells subpopulations in CD3E humanized mice and C57BL/6 mice. (B)Percentage of thymus CD4+ T cells, CD8 + T cells and Treg cells in TCRβ cells (n=4). (C) Flow cytometry pictures of spleen T cells subpopulations in CD3E humanized mice and C57BL/6 mice. (D)Percentage of spleen CD4+ T cells, CD8 + T cells and Treg cells in TCRβ cells. n=4 mice per group.

Fig.4 Proliferation of T cells isolated from WT and CD3E humanized mice under stimulation of CD3 and CD28

(A) Representative CFSE histograms showing proliferation of CD4+ T-cells and CD8+ T-cells under stimulation of mouse or human CD3 together with mouse CD28. (B) Percentage of CD4+ T-cells and CD8+ T-cells. n=4 mice per group.

Fig.5 Activation of T cells isolated from WT and CD3E humanized mice under stimulation of CD3 and CD28

(A) Representative flow plots of CD69 and CD25 expression showing activation of CD4+ T-cells and CD8+ T-cells under stimulation of mouse or human CD3 together with mouse CD28. (B) Percentage of activated CD4+ T cells and CD8+ T-cells. n=4 mice per group.

Fig. 6 The application of CD3E humanized mice in tumor immunotherapy

(A-B) Pharmacodynamic response to PD-1 monoclonal antibody and CD3E monoclonal antibody in C57BL/6 mice (A) and CD3E humanized mice (B). (C) Pharmacodynamic response to Blinatumomab in CD3E humanized mice. n=6 mice per group.

Fig. 7 Decrease in the proportion of T cells caused by CD3E antibody

(A) The percentage of B cells among the $CD45^+$ T cells. (B) The percentage of T cells among the $CD45^+$ T cells. (C) The percentage of $CD4^+$ T cells among the TCR-β^+ T cells. (D) The percentage of $CD8^+$ T cells among the TCR-β^+ T cells. n=6 mice per group. **: $p<0.01$, ***:$p<0.001$.

Figure 1

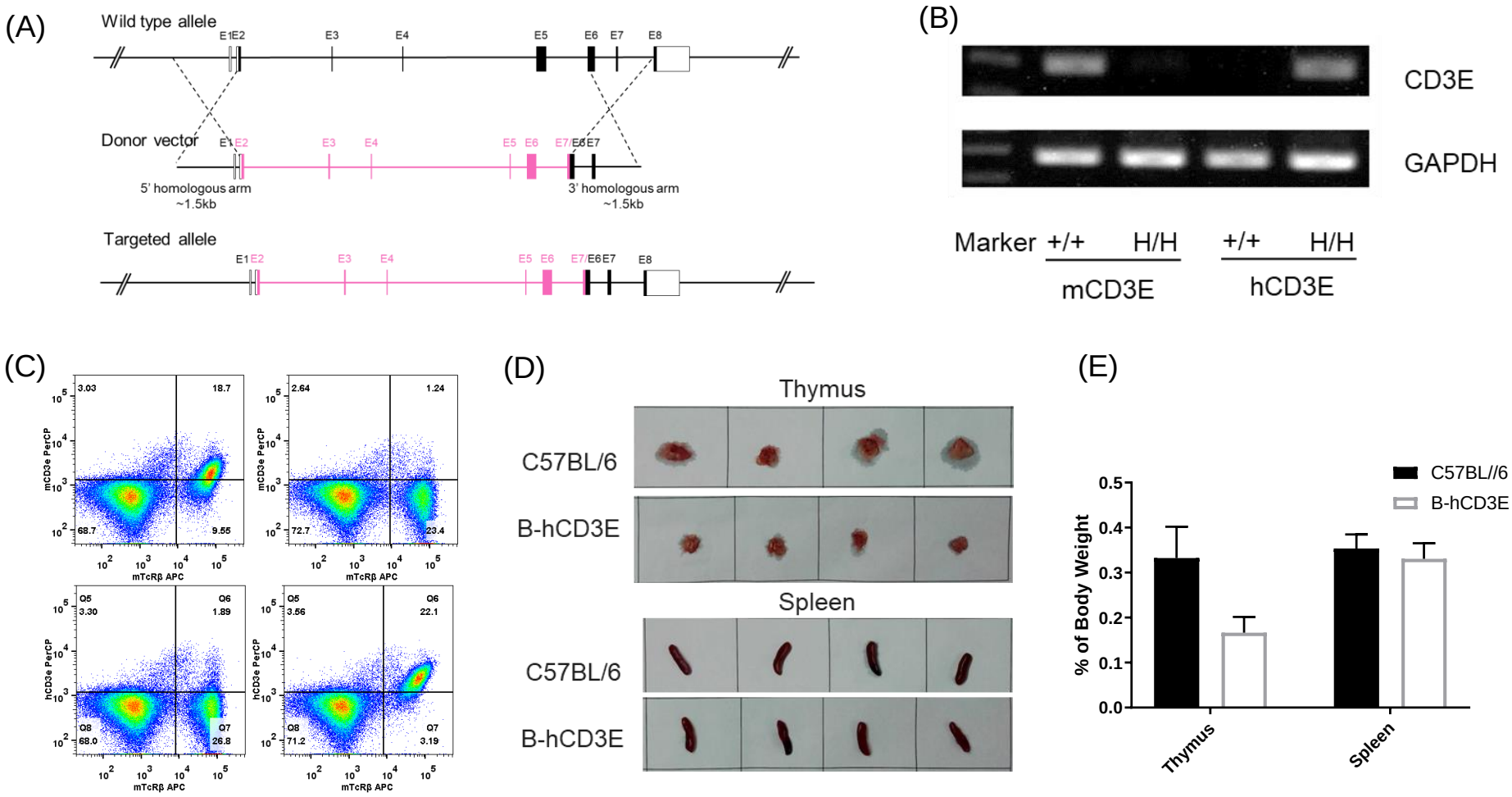
(A)
Wild type allele
E1E2
E3
E4
E5
E6
E7
E8
Donor vector
5' homologous arm
~1.5kb
3' homologous arm
~1.5kb
Targeted allele
(B)
CD3E
GAPDH
Marker
+/+
H/H
+/+
H/H
mCD3E
hCD3E
(C)
3.03
18.7
68.7
9.55
2.64
1.24
72.7
23.4
Q5
3.30
Q6
1.89
Q8
68.0
Q7
26.8
Q5
3.56
Q6
22.1
Q8
71.2
Q7
3.19
mTcRβ APC
mCD3e PerCP
hCD3e PerCP
(D)
Thymus
C57BL/6
B-hCD3E
Spleen
C57BL/6
B-hCD3E
(E)
C57BL//6
B-hCD3E
% of Body Weight
0.5
0.4
0.3
0.2
0.1
0.0
Thymus
Spleen

Figure 2

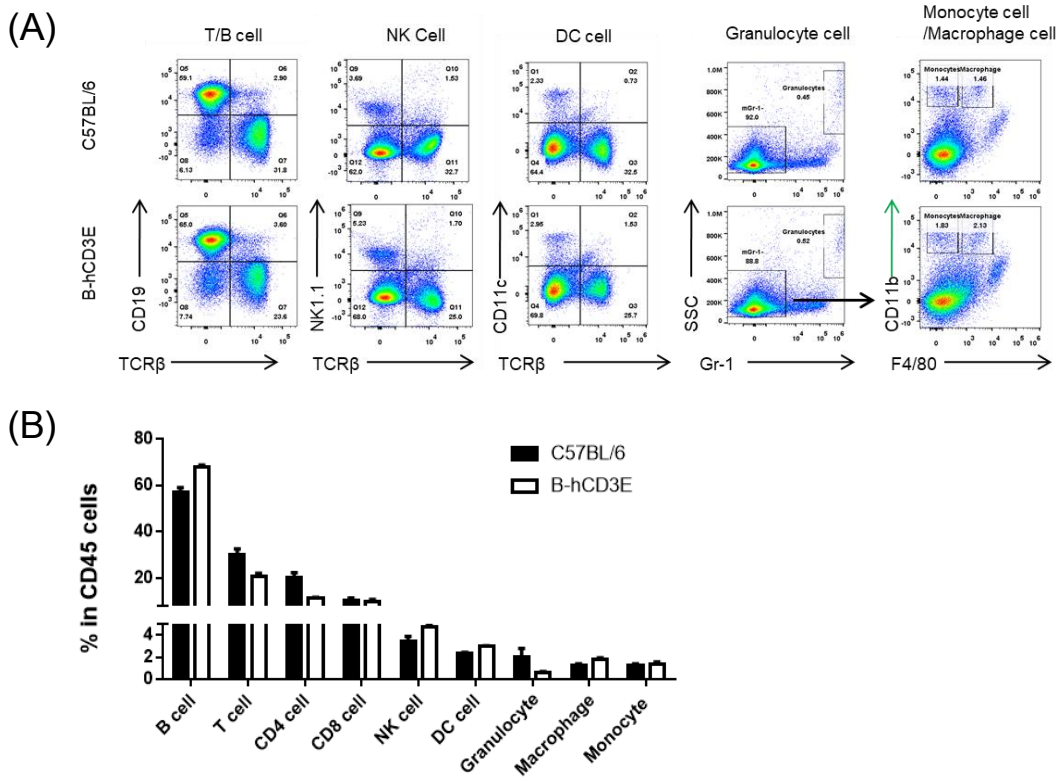
(A)
T/B cell
NK Cell
DC cell
Granulocyte cell
Monocyte cell
/Macrophage cell
C57BL/6
B-hCD3E
CD19
TCRβ
NK1.1
TCRβ
CD11c
TCRβ
SSC
Gr-1
CD11b
F4/80
(B)
% in CD45 cells
C57BL/6
B-hCD3E
B cell
T cell
CD4 cell
CD8 cell
NK cell
DC cell
Granulocyte
Macrophage
Monocyte

Figure 3

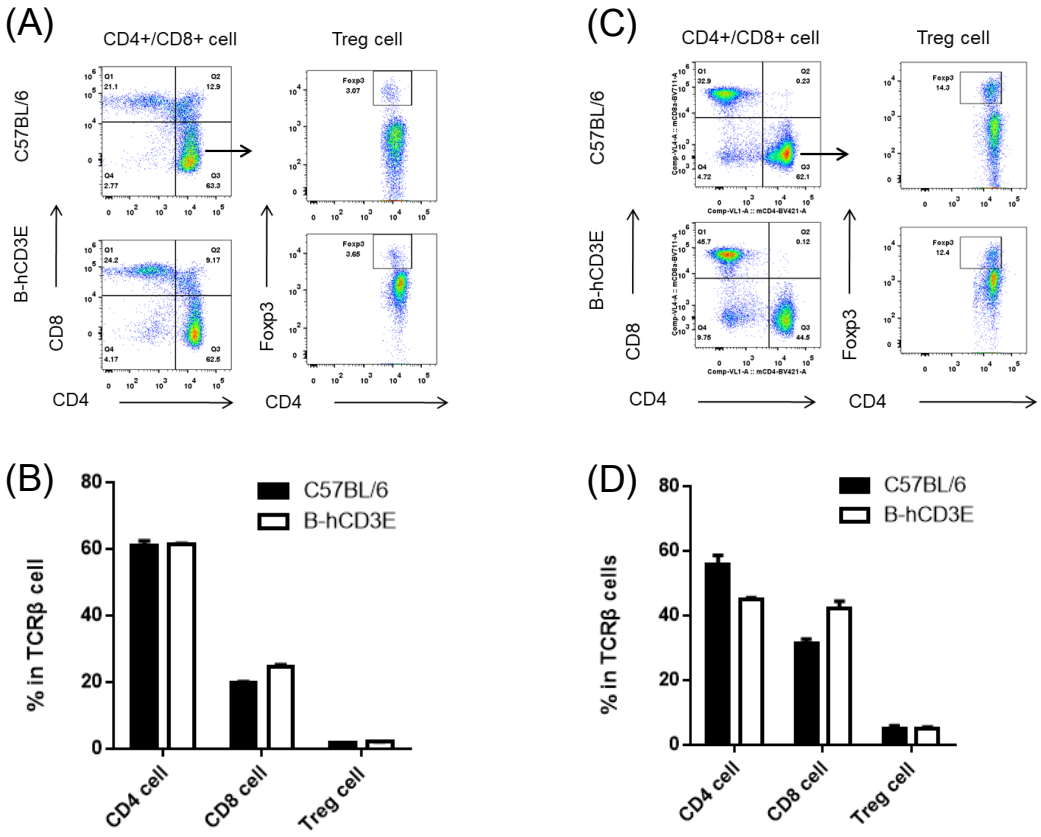
(A)
CD4+/CD8+ cell
Treg cell
C57BL/6
B-hCD3E
CD8
CD4
Foxp3
CD4
(C)
CD4+/CD8+ cell
Treg cell
C57BL/6
B-hCD3E
CD8
CD4
Foxp3
CD4
(B)
% in TCRβ cell
C57BL/6
B-hCD3E
CD4 cell
CD8 cell
Treg cell
(D)
% in TCRβ cells
C57BL/6
B-hCD3E
CD4 cell
CD8 cell
Treg cell

Figure 4

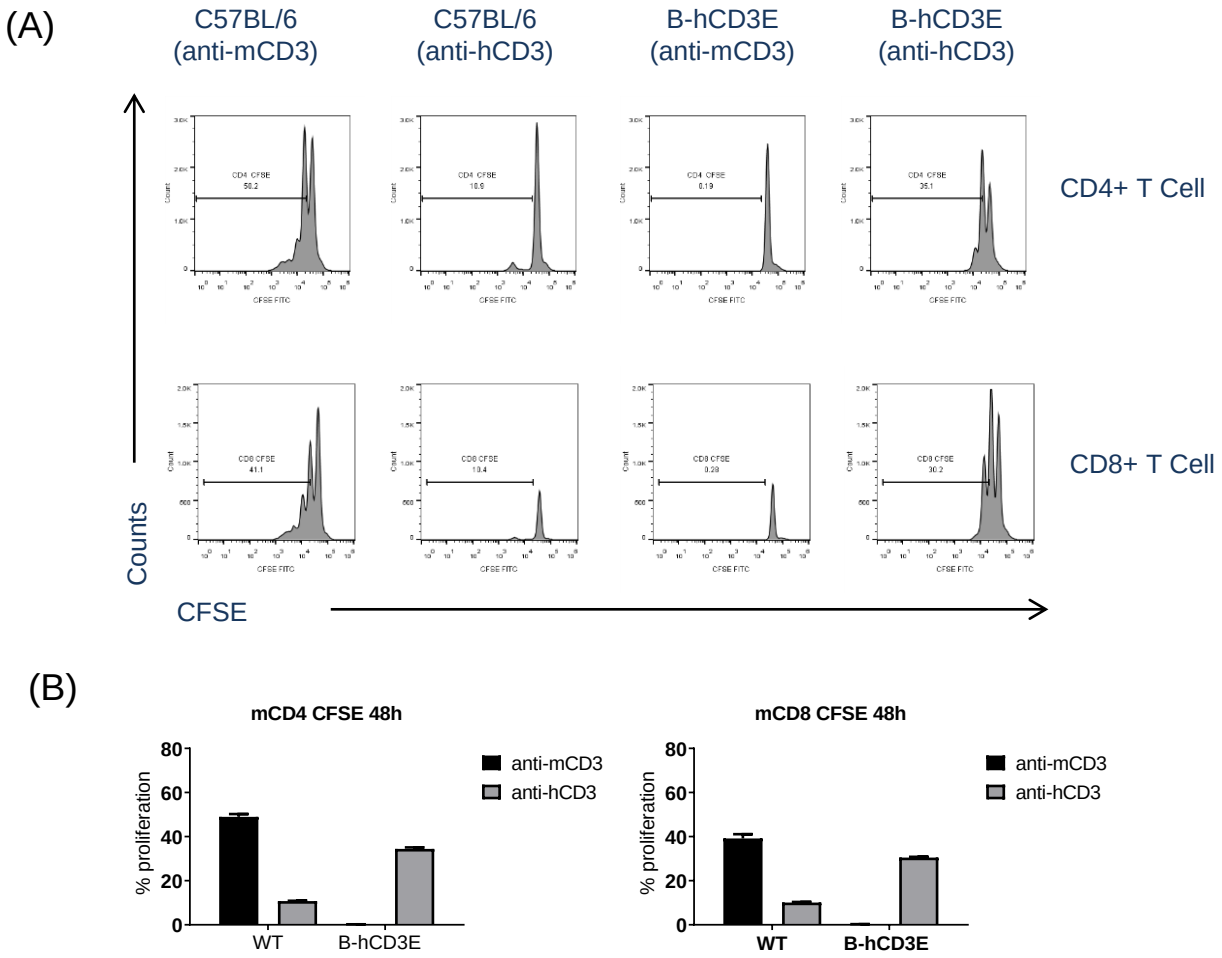
(A)
C57BL/6 (anti-mCD3)
C57BL/6 (anti-hCD3)
B-hCD3E (anti-mCD3)
B-hCD3E (anti-hCD3)
CD4+ T Cell
CD8+ T Cell
Counts
CFSE
(B)
mCD4 CFSE 48h
mCD8 CFSE 48h
% proliferation
anti-mCD3
anti-hCD3
WT
B-hCD3E

Figure 5

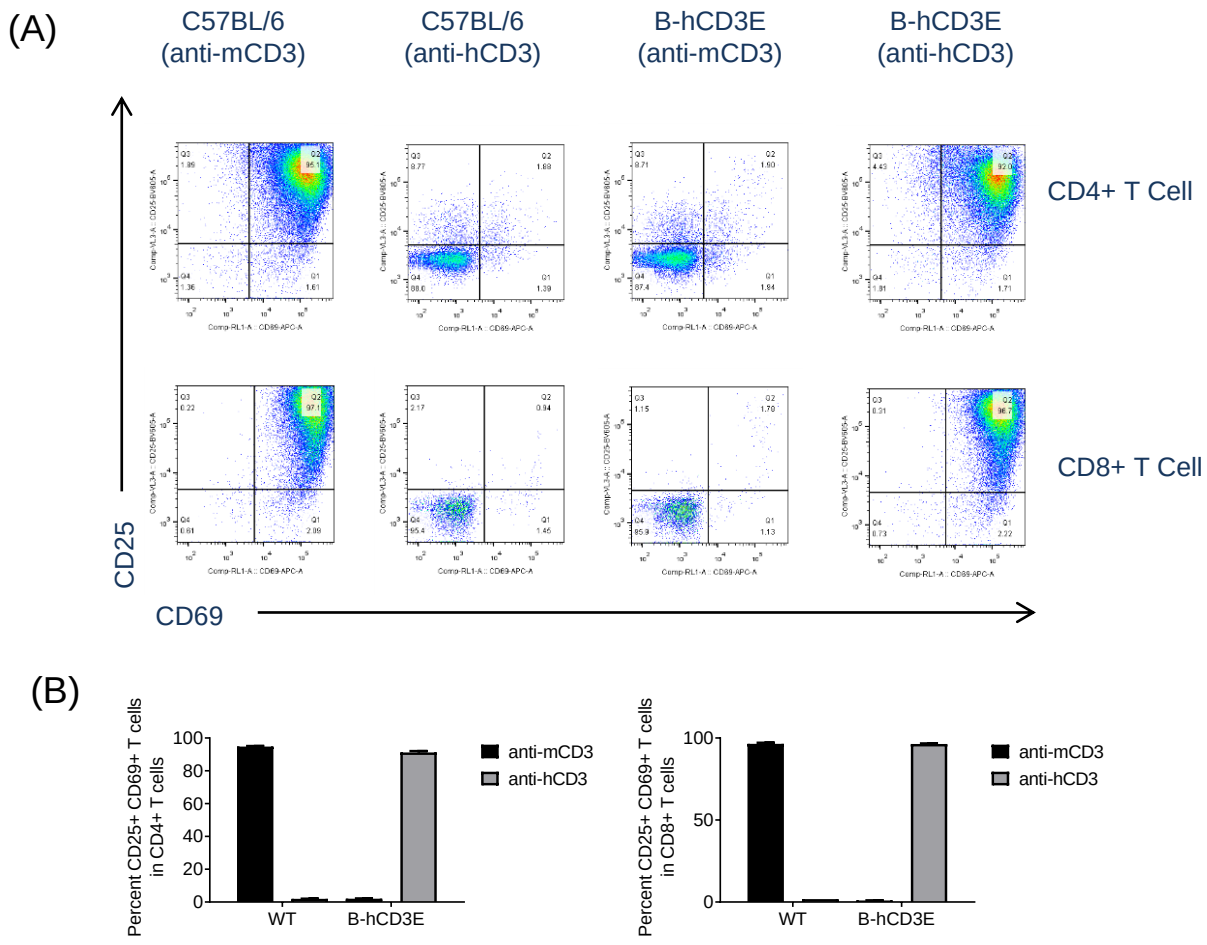
(A)
C57BL/6 (anti-mCD3)
C57BL/6 (anti-hCD3)
B-hCD3E (anti-mCD3)
B-hCD3E (anti-hCD3)
CD4+ T Cell
CD8+ T Cell
CD25
CD69
(B)
Percent CD25+ CD69+ T cells in CD4+ T cells
100
80
60
40
20
0
WT
B-hCD3E
anti-mCD3
anti-hCD3
Percent CD25+ CD69+ T cells in CD8+ T cells
100
50
0
WT
B-hCD3E
anti-mCD3
anti-hCD3

Figure 6

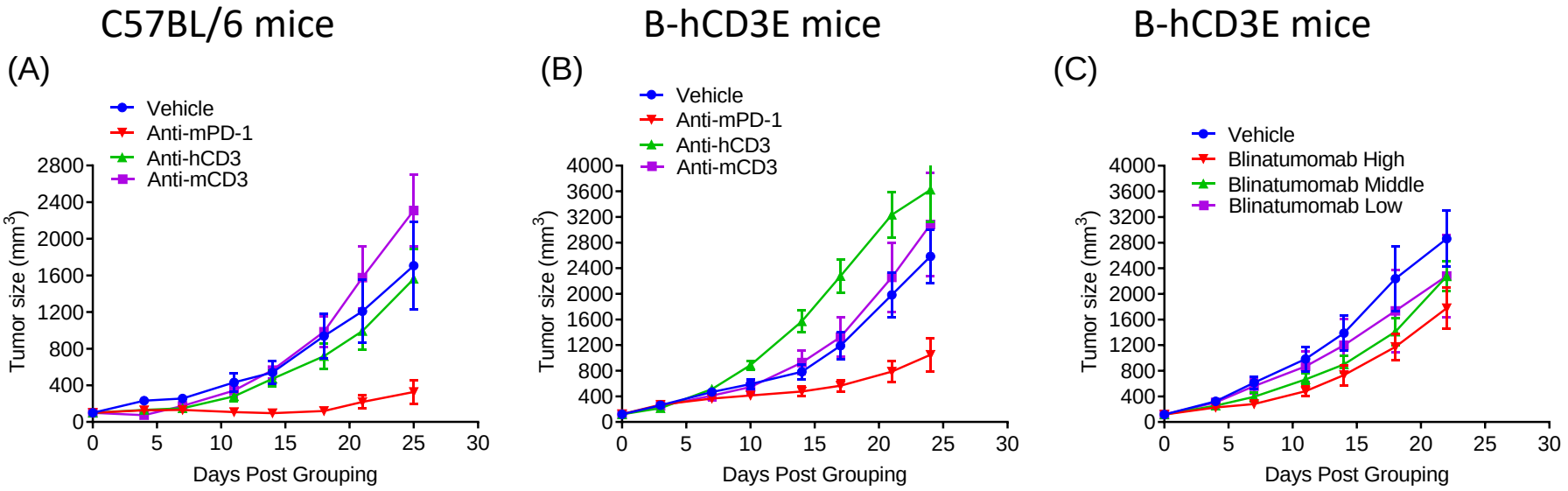
C57BL/6 mice
(A)
Vehicle
Anti-mPD-1
Anti-hCD3
Anti-mCD3
Tumor size (mm3)
Days Post Grouping
B-hCD3E mice
(B)
Vehicle
Anti-mPD-1
Anti-hCD3
Anti-mCD3
Tumor size (mm3)
Days Post Grouping
B-hCD3E mice
(C)
Vehicle
Blinatumomab High
Blinatumomab Middle
Blinatumomab Low
Tumor size (mm3)
Days Post Grouping

Figure 7

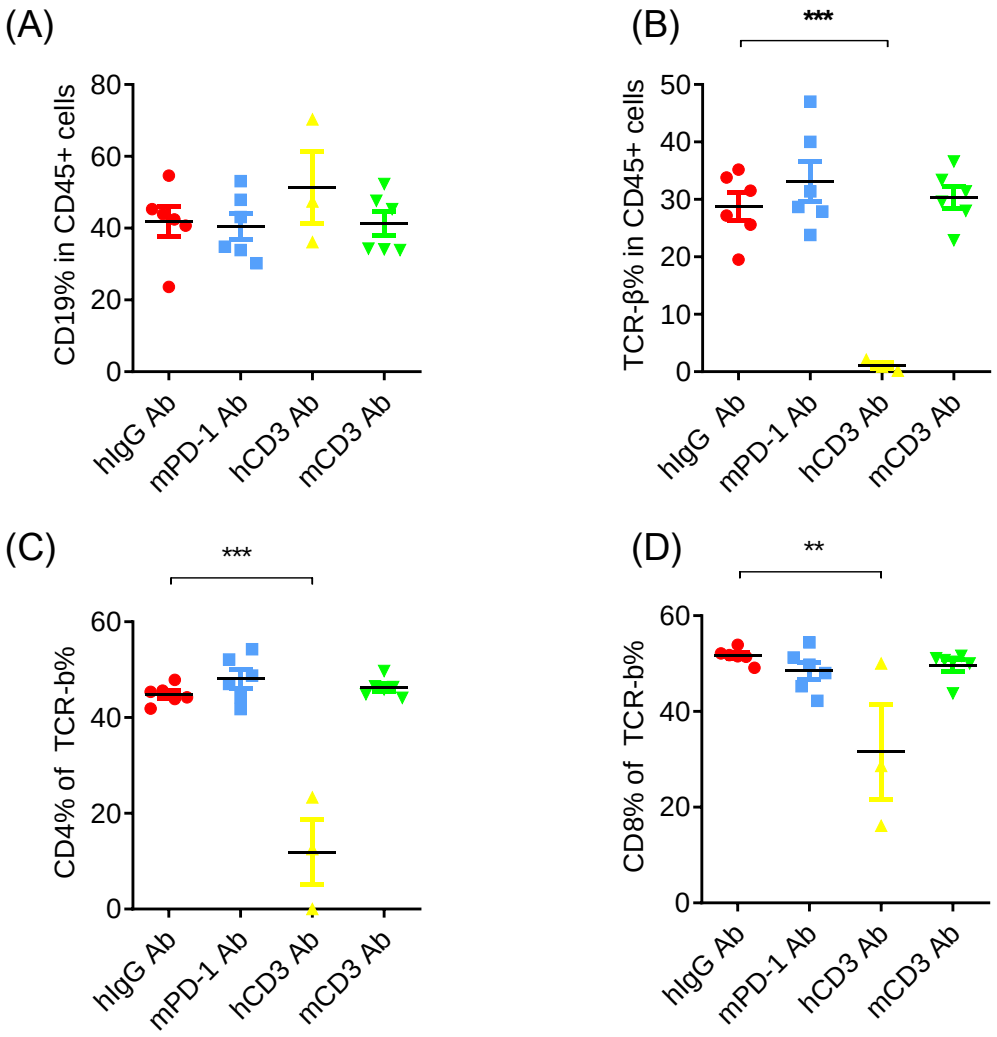
(A)
CD19% in CD45+ cells
80
60
40
20
0
hIgG Ab
mPD-1 Ab
hCD3 Ab
mCD3 Ab
(B)
***
TCR-β% in CD45+ cells
50
40
30
20
10
0
hIgG Ab
mPD-1 Ab
hCD3 Ab
mCD3 Ab
(C)
***
CD4% of TCR-b%
60
40
20
0
hIgG Ab
mPD-1 Ab
hCD3 Ab
mCD3 Ab
(D)
**
CD8% of TCR-b%
60
40
20
0
hIgG Ab
mPD-1 Ab
hCD3 Ab
mCD3 Ab

Supplementary Figure 1

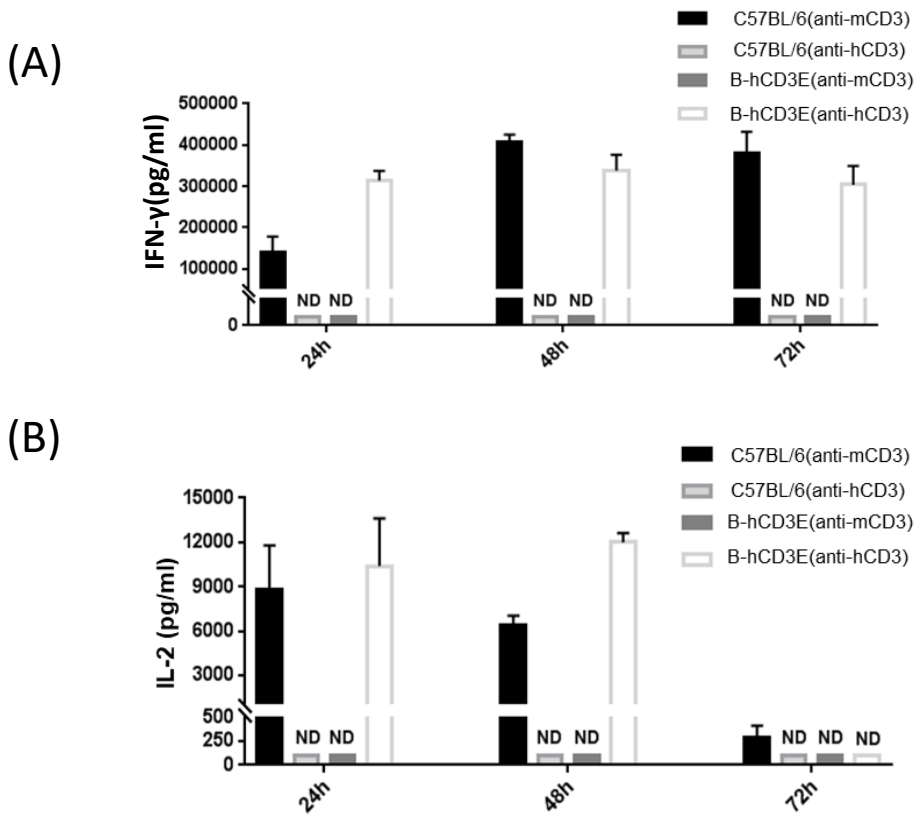

T cell activation stimulated with anti-CD3 antibody *in vitro*

(A) IFN-γ production under the stimulation of anti-CD3E antibody and anti-mCD28 antibody for 24h, 48h and 72h. (B) IL-2 production under the stimulation of anti-CD3E antibody and anti-mCD28 antibody for 24h, 48h and 72h. n=4 mice per group.